THE ASTROPHYSICAL JOURNAL, 593:L133–L136, 2003 August 20

MAGNETOHYDRODYNAMIC NUMERICAL SIMULATIONS OF SOLAR X-RAY JETS BASED ON THE MAGNETIC RECONNECTION MODEL THAT INCLUDES CHROMOSPHERIC EVAPORATION

TAKEHIRO MIYAGOSHI[1]
National Astronomical Observatory of Japan, 2-21-1 Osawa, Mitaka, Tokyo 181-8588, Japan; and the Graduate University for Advanced Studies, Hayama, Miura, Kanagawa 240-0193, Japan

AND

TAKAAKI YOKOYAMA[2]
National Astronomical Observatory of Japan, Nobeyama, Minamimaki, Minamisaku, Nagano 384-1305, Japan
Received 2002 December 17; accepted 2003 July 7; published 2003 July 16

ABSTRACT

We studied solar coronal X-ray jets by MHD numerical simulations with thermal conduction effects based on the magnetic reconnection model. Key physical processes are included, such as the emergence of magnetic fluxes from the convection zone, magnetic reconnection with the coronal magnetic fields, heat conduction to the chromosphere, and chromospheric evaporation. High-density evaporation jets were successfully reproduced in the simulations. The mass of the evaporation jets M is described as $M = 6.8 \times 10^{12}\ \mathrm{g}(B/10\ \mathrm{G})^{15/7}(T_{cor}/10^6\ \mathrm{K})^{5/14} \times (s_{flare}/5000\ \mathrm{km})^{12/7}(t/400\ \mathrm{s})$, where B is the magnetic field strength, T_{cor} is the coronal temperature, s_{flare} is the loop height, and t is the duration of the ejection.

Subject headings: MHD — Sun: corona — Sun: flares — Sun: magnetic fields — Sun: X-rays, gamma rays

1. INTRODUCTION

With the help of *Yohkoh*, the dynamic behavior of the solar corona has been revealed. *Solar coronal X-ray jets* are one of the most interesting phenomena (Shibata et al. 1992; Strong et al. 1992) and are observed as transitory X-ray enhancements with an apparent collimated motion (see Shimojo et al. 1996 for *Yohkoh* observation). Shibata et al. (1994) proposed a phenomenological model of the X-ray jets. Based on the frequent observation of X-ray jets from emerging flux regions, they considered that the plasma in the jets is accelerated and heated by the magnetic reconnection between the emerging flux and the preexisting coronal magnetic field. Yokoyama & Shibata (1995, 1996) performed two-dimensional MHD simulations based on this scenario and succeeded in reproducing a plasma-collimated flow along magnetic fields. However, their simulations could not explain the observed density. This is probably because their simulation did not include the effect of conduction and thus evaporation. Shimojo et al. (2001) performed one-dimensional hydrodynamic simulations with the conduction effect and succeeded in reproducing the dense flow in X-ray jets under the assumption that the energy input is a given function of time. However, the energy-release process (i.e., the magnetic reconnection) is not treated in the simulation by Shimojo et al. (2001). We need to combine the simulations by Yokoyama & Shibata and by Shimojo et al. to study the observed properties self-consistently. In this Letter, we include the heat conduction effect and the chromospheric evaporation process, which were neglected in Yokoyama & Shibata (1995, 1996). The energy-release process by means of the magnetic reconnection between the emerging flux and the coronal fields is solved self-consistently; this was neglected in Shimojo et al. (2001) because their work was one-dimensional and because the energy was given artificially. Key processes of the reconnection model are all included, such as the emerging flux from the convection zone, the magnetic reconnection to coronal fields, the heat conduction to the chromosphere, and the plasma evaporation process. Based on the simulation results, we derived the formula describing the jet mass as a function of the quiet coronal parameters.

[1] Current address: Kwasan Observatory, Kyoto University, Omine-chou, Kitakazan, Yamashina-ku, Kyoto 607-8471, Japan; miyagosi@kwasan.kyoto-u.ac.jp.
[2] Current address: Department of Earth and Planetary Science, University of Tokyo, 7-3-1 Hongo, Bunkyo-ku, Tokyo 113-0033, Japan; yokoyama.t@eps.s.u-tokyo.ac.jp.

2. MODEL OF NUMERICAL SIMULATIONS

We solve the nonlinear, time-dependent, resistive, compressible MHD equations. A rectangular computation box with two-dimensional Cartesian coordinates in the (x, z)-plane is assumed. The surface of the Sun is at $z = 0$. The y-component of the partial derivative $\partial/\partial y$ is neglected, although the velocity V_y and magnetic field B_y are included. The medium is assumed to be an inviscid perfect gas with a specific heat ratio of $\gamma = 5/3$. Gravitational acceleration is assumed to be uniform in the negative z-direction. An anomalous resistivity model is assumed, as described later. Ohmic heating and the heat conduction effect are taken into account. The conduction coefficient is a Spitzer-type one that is proportional to $T^{5/2}$, where T is temperature. We also assume that it is anisotropic, working only in the direction along the magnetic field line so that $\kappa \approx \kappa_\parallel = \kappa_0 T^{5/2}$ (where $\kappa_0 \approx 10^{-6}$ ergs s^{-1} cm^{-1} K$^{-7/2}$) and $\kappa_\perp = 0$ in the simulations, where $\kappa_\parallel$ and $\kappa_\perp$ are the conductivity along and across the magnetic field, respectively. The units of length, velocity, time, density, and temperature in the simulations are H, C_{s0}, $\tau \equiv H/C_{s0}$, ρ_0, and T_0 respectively, where H, C_{s0}, ρ_0, and T_0 are the pressure scale height, sound speed, density, and temperature of the photosphere in the initial state, respectively.

The gas is in magnetohydrostatic equilibrium in the initial state. The gas consists of three layers: From top to bottom, a hot layer ($z \geq 8$, the corona), a cool layer ($0 \leq z \leq 8$, the photosphere/chromosphere), and a convection layer ($z \leq 0$, the convection zone). The ratio of the coronal temperature to the photospheric temperature (T_{cor}/T_0) is 100 for a typical case. In the convection layer, we took $T(z) = T_0 - (a|dT/dz|_{ad})z$, where $|dT/dz|_{ad} \equiv (\gamma - 1)/\gamma$ is the adiabatic temperature gradient and a is the dimensionless constant of order unity. Here we took $a = 2.0$ (note that when $a > 1$, the convection zone becomes

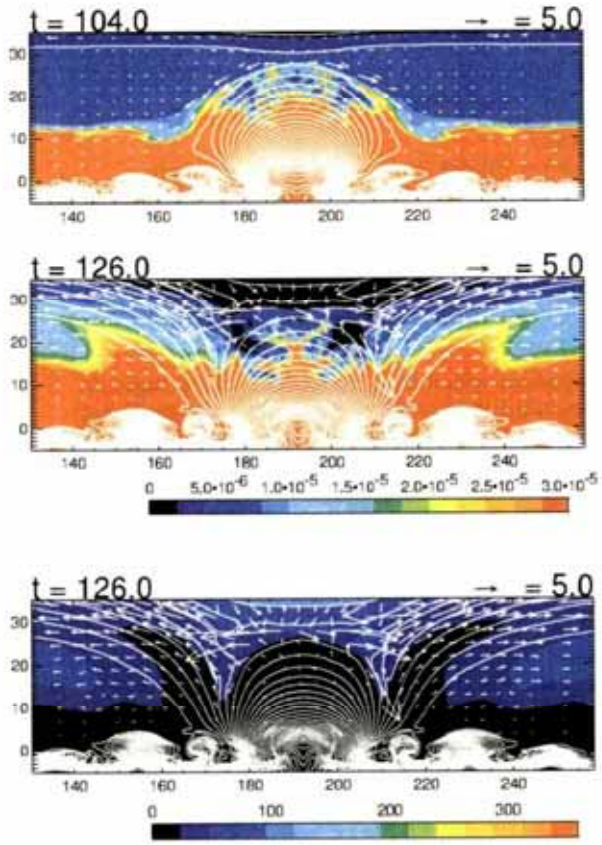

FIG. 1.—Simulation results for a typical case. The color map shows the density (*top panel and middle panel*) and the temperature (*bottom panel*); the white lines show the magnetic lines of force; and the white arrows show the velocity field.

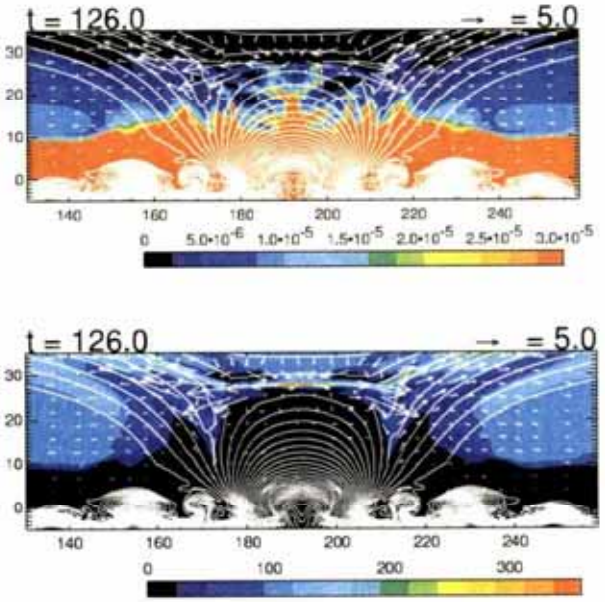

FIG. 2.—Same as Fig. 1, but without the heat conduction effect. A density map (*top panel*) and a temperature map (*bottom panel*) are shown. In this case, the magnetic reconnection occurs, but the dense jet flow is not formed.

unstable in the convective Parker instability). The initial magnetic field consists of two parts: a flux sheet in the convection layer and a nearly uniform field in the hot layer. We took the plasma beta of the flux sheet in the convection zone as $\beta_{i0} = 4$ and the coronal magnetic field as $\beta_{cor} = 0.1$ for a typical case. (The schematic picture of the initial configuration and the distribution of each physical value as a function of z are given in Fig. 2 of Yokoyama & Shibata 1996). In order to excite the convective Parker instability (Parker 1966; Nozawa et al. 1992), a small velocity perturbation in the z-direction with an amplitude of 5% of the local sound speed was imposed on the magnetic flux sheet within a finite domain. We took the wavelength of the perturbation to be 20, which is nearly the most unstable wavelength of the linear Parker instability. The resistivity is determined self-consistently from the local value of the current density for every time step. It is described as $\eta = 0$ for $v_d < v_c$ and as $\eta = \alpha(v_d/v_c - 1)$ for $v_d \geq v_c$, where $\alpha = 0.01$ is the resistivity parameter, $v_d \equiv J/\rho$ is the (relative ion-electron) drift velocity, $v_c = 1000$ is the threshold above which anomalous resistivity sets in, and $J = J_x^2 + J_y^2 + J_z^2$ is the total current density. [In dimensional form, $v_d \equiv J/(en)$, where e is the elementary electric charge and n is the particle number density.] We also assumed that there is an upper limit, $\eta < \eta_{max} = 1.0$.

In the numerical procedures, the modified Lax-Wendroff method is used for the MHD part of the calculations, and the red and black overrelaxation method is adopted for the heat conduction part (e.g., Hirsch 1989, p. 476; Yokoyama & Shibata 2001). The number of grid points is 550 × 500. We adopt nonuniform grid sizes. The minimum grid sizes are $\Delta x = 0.25$ and $\Delta z = 0.15$. For the boundaries, we assumed a periodic condition for $x = x_{min}$ and $x = x_{max}$, a symmetric (rigid conducting wall) condition for $z = z_{min}$, and a free condition for $z = z_{max}$. Here $x_{min} = 0$, $x_{max} = 390$, $z_{min} = -5$, and $z_{max} = 265$.

3. RESULTS

Figure 1 shows the simulation results. The top and middle panels show the density (*color map*), magnetic lines of force (*white lines*), and velocity fields (*white arrows*). Initially, the magnetic flux in the convection layer rises because of the Parker instability, and it evolves to form a magnetic loop in the atmosphere (Fig. 1, *top panel*). A gravitational downflow occurs along the rising loop (e.g., Shibata et al. 1989). When the top of the rising loops reaches the level of the coronal fields, a current sheet is created between the loop top and the coronal field. As the emerging motion continues, the current sheet becomes thinner, and the current density increases. Then magnetic reconnection starts when the critical condition for the anomalous resistivity is satisfied. This is the Petschek-type reconnection (e.g., Petschek 1964; Yokoyama & Shibata 1994) because the diffusion region is spatially localized and because the high-temperature plasma is produced by slow shocks. Magnetic energy is converted into thermal energy through shocks. Then the thermal energy is transported to the chromosphere along the magnetic fields by heat conduction. It causes the "chromospheric evaporation" (e.g., Hirayama 1974). The dense gas of the chromosphere rises up along the reconnected magnetic fluxes by evaporation, and a pair of jets are ejected in the left and right directions (Fig. 1, *middle panel*). The density of the jets is ~10 times as large as that of the surrounding gas. This is almost consistent with the *Yohkoh* observations (Shimojo & Shibata 2000). Figure 2 shows the numerical simulation results without the heat conduction effects. From a comparison

of Figure 2 with Figure 1, it is found that the heat conduction effect is essential for reproducing the high-density jets.

By including the heat conduction effect, the temperature of the reconnection region becomes lower than that of the quiet corona. Therefore, this simulation succeeded in reproducing the enhancement of the density but failed to reproduce the enhancement of the temperature in the observed jets (Shimojo & Shibata 2000). The reason for the low temperature is that the cooling by conduction is more efficient than the heating by magnetic reconnection. But if the magnetic field is as strong as that of the real corona, the released thermal energy via magnetic reconnection may increase; in consequence, the heating rate becomes larger than the cooling rate, and the temperature should be higher.

Figure 3 shows the total mass of the evaporated plasma as a function of the coronal parameters. The studied parameters are the coronal magnetic field strength B (*top panel*), the conduction coefficient κ_0 (*middle panel*), and the initial coronal temperature T_{cor} (*bottom panel*). From these results, it is found that the evaporated mass is described as

$$M \propto \kappa_0^{2/7} B^{15/7} T_{cor}^{5/14}. \tag{1}$$

Note that although κ_0 itself is a universal constant, its value changes in the simulations as the normalization unit changes.

The analytical expression of the mass of the evaporation jets is derived by Shimojo et al. (2001). Their equation (19) is as follows:

$$M \sim \frac{\gamma - 1}{\gamma} \frac{m_p \kappa_0^{2/7} F_h^{5/7} S}{2 k_B s_{flare}^{2/7}} t, \tag{2}$$

where k_B is the Boltzmann constant, m_p is the proton mass, F_h is the heating rate in the energy release region, s_{flare} is the loop height, S is the cross section of the loop, and t is the time from the start of the energy deposition. (Note that here we assume that the height of the reconnection region and the loop height are almost equal because reconnection occurs at the loop top.) Here we extend the model of Shimojo et al. (2001) by including the effect of magnetic reconnection. The heating rate F_h can be regarded as the energy release rate into the reconnection region and can be approximated as

$$F_h \sim M_A \frac{B^2}{8\pi} V_A \sim M_A \frac{B^3}{8\pi} \frac{\sqrt{k_B}}{\sqrt{4\pi m_p}} \frac{\sqrt{T_{cor}}}{\sqrt{p_{cor}}}, \tag{3}$$

where V_A is the Alfvén speed of the reconnection inflow region, M_A is the Alfvén Mach number of the reconnection inflow, and p_{cor} is the coronal gas pressure. Using equations (2) and (3), the mass becomes

$$M \sim \frac{\gamma - 1}{\gamma} \frac{M_A^{5/7} m_p^{9/14}}{2 k_B^{9/14} s_{flare}^{2/7}} \kappa_0^{2/7} B^{15/7} T_{cor}^{5/14} p_{cor}^{-5/14} St. \tag{4}$$

To compare this analytical model with the simulation results, this formula is normalized and becomes

$$M' \sim \frac{\gamma - 1}{2\gamma} \kappa_0'^{2/7} B'^{15/7} T_{cor}'^{5/14} s_{flare}'^{-2/7} p_{cor}'^{-5/14} S' t', \tag{5}$$

where the primed values are nondimensional. The dashed lines in Figure 3 indicate this relationship. There is a good agreement between the simulations and the analytical model. We should note that the coverage of the dynamical range for the magnetic field strength is less than 1 order of magnitude. This is not enough to compare with the theoretical explanations. But the strongest magnetic strength shown in Figure 3 is almost at the upper limit for which our simulation code will work properly (i.e., without numerical overflows) by the present resources of our computer. We need higher resolution simulations to extend this range in order to strongly confirm our theoretical explanations.

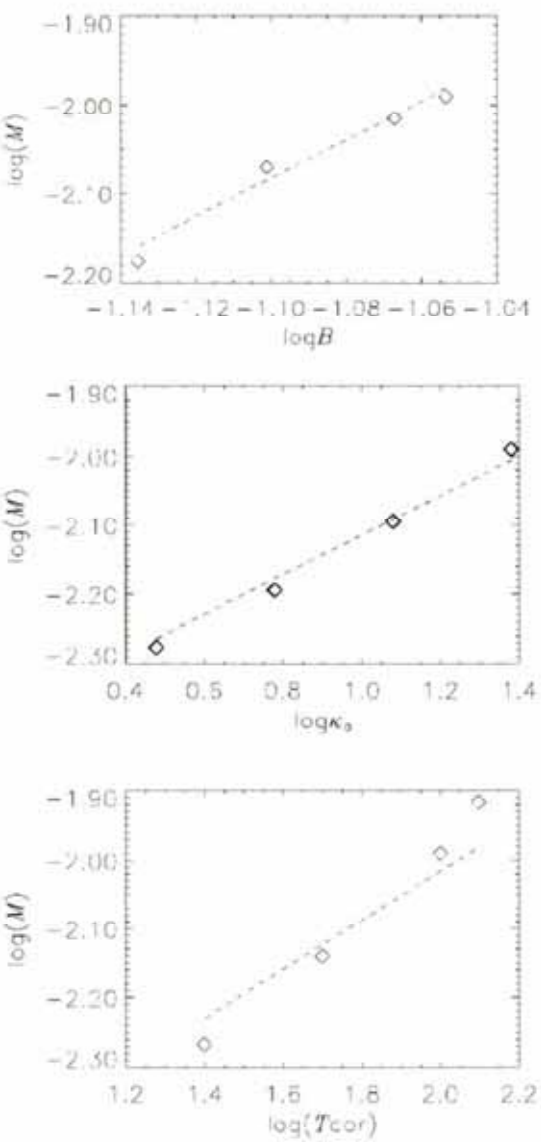

FIG. 3.—Evaporation jet mass (*vertical axis*) as a function of the magnetic fields strength (*top*), the conduction coefficient (*middle*), and the coronal temperature (*bottom*). The diamonds show the simulation results, and the dashed line shows the theoretical relation $M \propto \kappa_0^{2/7} B^{15/7} T_{cor}^{5/14}$.

4. DISCUSSIONS

In this Letter, we performed MHD simulations of coronal jets and included all the key processes (emerging flux, reconnection, conduction, and evaporation) based on the reconnection model by Shibata et al. (1994). We derived the dependence of the mass of the evaporation jets on the coronal variables,

as shown in equation (4). With the typical values of the corona, this is described as

$$M = 6.8 \times 10^{12}\ \mathrm{g} \left(\frac{B}{10\ \mathrm{G}}\right)^{15/7} \left(\frac{T_{\mathrm{cor}}}{10^6\ \mathrm{K}}\right)^{5/14} \times \left(\frac{s_{\mathrm{flare}}}{5000\ \mathrm{km}}\right)^{12/7} \left(\frac{t}{400\ \mathrm{s}}\right). \quad (6)$$

Here we assume that the cross section of a jet is approximated as $S \approx s_{\mathrm{flare}}^2$. From observations, the number density of jets is $(0.7\text{–}4.0) \times 10^9\ \mathrm{cm}^{-3}$, and the number density of the footpoint flares is $(2.4\text{–}10.0) \times 10^9\ \mathrm{cm}^{-3}$ (Shimojo & Shibata 2000). From equation (6), the value of the density of the jet n_{jet} can be derived as $n_{\mathrm{jet}} = M/(m_p V)$, where V is the volume of the jet. If the aspect ratio (length over width) of the jet is $\alpha \sim 7$ (see Shimojo et al. 1996, 2000), the volume is $V \sim \alpha s_{\mathrm{flare}}^3 \sim 8.8 \times 10^{26}\ \mathrm{cm}^3$. Then we obtain $n_{\mathrm{jet}} \approx 4.5 \times 10^9\ \mathrm{cm}^{-3}$. This is consistent with the observed values.

From the simulation results, we found that the gas pressure in the jet flow balances with the total (gas and magnetic) pressure of the surrounding gas. Therefore, we consider that the jet temperature is determined by this balance. This balance is described as $p_{\mathrm{jet}} = p_{\mathrm{cor}} + B^2/8\pi$, where p_{jet} is the gas pressure of the jet, p_{cor} is the gas pressure of the outside region, and B is the magnetic field strength of the outside region. This is because the magnetic pressure along the jets is very weak. Let us suppose that $n_{\mathrm{cor}} = 10^9\ \mathrm{cm}^{-3}$, $T_{\mathrm{cor}} = 10^6$ K, $B = 10$ G, and $n_{\mathrm{jet}} = 4.5 \times 10^9\ \mathrm{cm}^{-3}$, where n_{cor} is the number density of the outside coronal gas and T_{cor} is the temperature of the outside one. Using these values and the total pressure balance equation, we get $T_{\mathrm{jet}} = 6.7 \times 10^6$ K, where T_{jet} is the temperature of the jet. This is almost consistent with the observations (3–8 MK, with an average of 5.6 MK; see Shimojo & Shibata 2000).

We are grateful to Professor K. Shibata and M. Shimojo for their helpful discussions. The numerical computations were carried out on VPP5000 at the Astronomical Data Analysis Center of the National Astronomical Observatory, Japan, which is an interuniversity research institute of astronomy operated by the Ministry of Education, Culture, Sports, Science, and Technology.

REFERENCES

Hirayama, T. 1974, Sol. Phys., 34, 323
Hirsch, C. 1989, Numerical Computation of Internal and External Flows, Vol. 1: Fundamentals of Numerical Discretization (New York: Wiley)
Nozawa, S., Shibata, K., Matsumoto, R., Tajima, T., Sterling, A. C., Uchida, Y., Ferrari, A., & Rosner, R. 1992, ApJS, 78, 267
Parker, E. N. 1966, ApJ, 145, 811
Petschek, H. E. 1964, in The Physics of Solar Flares, ed W. N. Hess (NASA SP-50; Washington, DC: NASA), 425
Shibata, K., et al. 1992, PASJ, 44, L173
Shibata, K., Nitta, N., Matsumoto, R., Tajima, T., Yokoyama, T., Hirayama, T., & Hudson, H. 1994, in Proc. Int. Symp. on the *Yohkoh* Scientific Results, X-Ray Solar Physics from *Yohkoh*, ed Y. Uchida, T. Watanabe, K. Shibata, & H. S. Hudson (Tokyo: Universal Academy Press), 29
Shibata, K., Tajima, T., Steinolfson, R. S., & Matsumoto, R. 1989, ApJ, 345, 584
Shimojo, M., Hashimoto, S., Shibata, K., Hirayama, T., Hudson, H. S., & Acton, L. 1996, PASJ, 48, 123
Shimojo, M., & Shibata, K. 2000, ApJ, 542, 1100
Shimojo, M., Shibata, K., Yokoyama, T., & Hori, K. 2001, ApJ, 550, 1051
Strong, K., Harvey, K. L., Hirayama, T., Nitta, N., Shimizu, T., & Tsuneta, S. 1992, PASJ, 44, L161
Yokoyama, T., & Shibata, K. 1994, ApJ, 436, L197
———. 1995, Nature, 375, 42
———. 1996, PASJ, 48, 353
———. 2001, ApJ, 549, 1160